

doi: 10.5862/MCE.66.4

Distribution capacity of sandy soils reinforced with geosynthetics

Распределяющая способность песчаных грунтов, армированных геосинтетикой

*A.S. Aleksandrov,
A.L. Kalinin,
M.V. Tsyguleva*

*Siberian State Automobile And Highway Academy,
Omsk, Russia*

Канд. техн. наук, доцент

*А.С. Александров,
аспирант А.Л. Калинин,
преподаватель М.В. Цыгулева,*

*Сибирская государственная автомобильно-
дорожная академия, г. Омск, Россия*

Key words: stress dispersion angle; load distribution angle; geosynthetics; reinforcement of soil basements; distributing ability; colour strip analysis

Ключевые слова: рассеивания напряжений; угол распределения нагрузки; геосинтетика; армирование грунтовых оснований; распределяющая способность; метод цветных полосок

Abstract. A review of shear strength analysis methods for ground bases reinforced with geosynthetics is given in the article. An angle of stress dispersion has been found to be the parameter of soils and discrete materials which were calculated according to the experimental data. The analysis of mathematical models that connect the angle of stress dispersion with other soil parameters which are ascertained in the laboratory was performed. This analysis shows the absence of direct experimental methods for investigation of distribution capacity. For this reason indirect measurements are used to calculate the angle of stress dispersion. The direct method for measuring distribution capacity has been developed on the basis of a colour strip analysis. There are two variants. The first way deals with photo interpretation, the second one uses full-scale models for direct measurements. Statistical analysis shows that reinforcement of ground bases increases distribution capacity of the soil under the geosynthetics.

Аннотация. В статье выполнен обзор методов расчета грунтовых оснований, армированных геосинтетическими материалами по сопротивлению сдвигу. Установлено, что угол рассеивания напряжений является параметром грунтов и дискретных материалов, определяемым по данным эксперимента. Выполнен анализ математических моделей связывающих угол рассеивания напряжений с другими параметрами грунтов, которые определяются в лаборатории. На основе этого анализа показано, что прямые методы экспериментального исследования распределяющей способности отсутствуют. Поэтому угол рассеивания напряжений вычисляют по данным косвенных измерений. Применением метода цветных полосок разработан прямой метод исследования распределяющей способности. Предложено два способа измерения распределяющей способности грунта. Первый способ состоит в обработке фотоизображений, а второй – заключается в прямых измерениях, выполняемых на натуральных моделях. Статистическая обработка результатов эксперимента показало, что армирование грунтовых оснований улучшает распределяющую способность грунта расположенного под геосинтетикой.

Introduction

A model of distribution capacity is based on the idea that load is distributed over the area which increases with depth [1]. Load in a ground elastic plastic half-space is distributed at the certain angle α_σ which is called angle of stress dispersion or angle of load distribution (Fig. 1).

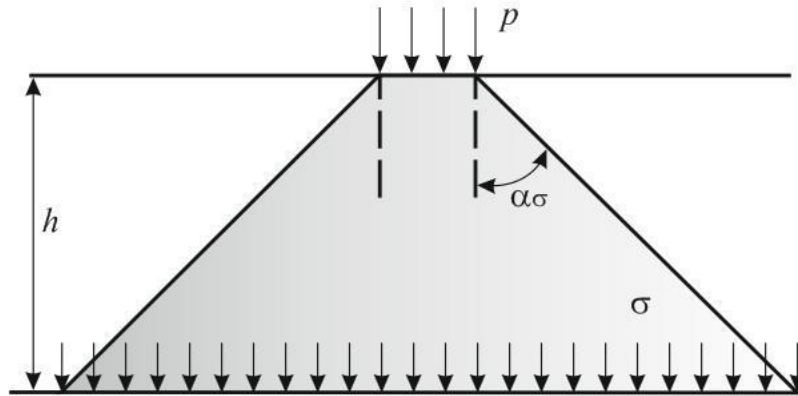


Figure 1. An original model of distribution capacity [1]

As it follows from the analysis of Figure 1, the pressure change with depth is determined by increasing the load distribution area. Consequently, vertical normal stress decreases and is calculated using the formula [1]

$$\sigma_z = p \cdot \left(1 + \frac{2 \cdot Z}{D_0} \cdot \operatorname{tg} \alpha_{\sigma} \right)^{-2}, \quad (1)$$

where p – pressure on the half-space surface, Pa; Z – depth plotted along the load symmetry axis from the surface to the point where the pressure is calculated, m; D_0 – diameter of a round plate under the load distributed on the half-space surface, m; α_{σ} – angle of stress dispersion, deg.

Since the directions of principal and coordinate axes coincide in the load symmetry axial section, formula (1) can be used to calculate the maximum principal stress in the ground half-space [2–6]. It is sufficient to substitute the dependent variable σ_z for the maximum principal stress σ_1 .

For the calculations of stresses in a finite thickness layer to be done, Odermark's method can be used. It was offered in 1949 but nowadays it is often applied in order to solve a wide variety of road structural analysis problems [3–11]. Thus, a combination of the idea of relationship (1) with Odermark's method makes it possible to design road structures.

As for some foreign countries, a model of distribution capacity is used to compute the limiting pressures upon the ground base. While developing methods of limiting pressure calculation using the model of distribution capacity, dyadic and trinomial relationships are deduced. They are similar to the Prandtl-Reisner and Terzaghi formulae that have the parameter connected with an angle of stress dispersion [12]. Creation of geosynthetics and its application for soil reinforcement necessitated the analysis of such structures. For this purpose, methods of limiting pressure determination based on a model of distributing capacity were used [13]. According to such methods, structures with geosynthetics are supposed to have a larger angle of stress dispersion compared with unreinforced structures with the layers of the same material and thickness [14–19]. Besides, the method proposed in [20] allows deriving a formula for calculation of the first critical load applied to the road base of the particulate material or to the subgrade soil using the relationship (1). An important element of all described methods is experimental determination of an angle of stress dispersion.

Indirect methods of determining the angle of stress dispersion are currently known. This characteristic is calculated using some other parameters: angle of repose [1], undrained shear strength [19, 20], etc. B.S. Radovsky reports that Ye. Golovachev believed the angle of stress dispersion α_{σ} to be equal to the angle of repose β_{or} [1]. This assumption can be written as

$$\alpha_{\sigma} = \beta_{\text{or}}. \quad (2)$$

The main problem of the relationship (2) is that the angle of repose can easily be calculated only for sandy loose soils. That is why equation (2) can not be used to find α_{σ} in clay and sandy compacted soils.

V.N. Gusev noticed that the angle of stress dispersion was influenced by consistency of the soil and he suggested that angle α_{σ} could be calculated by the formula

$$\alpha_{\sigma} = \alpha_{\sigma p} + s \cdot t, \quad (3)$$

where $\alpha_{\sigma p}$ – angle of load distribution (stress dispersion) in loose medium, deg; s – coefficient of medium material; t – shearing strength within the layer.

As for the relationship (3), it is rather difficult to calculate the angle of stress dispersion in loose medium $\alpha_{\sigma p}$. Thus, it makes sense to combine the ideas of Golovachev and Gusev and the angle α_{σ} can be calculated by the formula

$$\alpha_{\sigma} = \beta_1 + s \cdot t, \quad (4)$$

where β_1 – angle of repose of loose medium, deg.

The analysis of the relationship (4) shows that in order to calculate the angle of stress dispersion it is necessary to set up two experiments and to determine two parameters: angle β_1 and strength t . Besides, the coefficient s should also be determined as it is different for various soils.

Formulae connecting undrained shear strength with load parameters and angle of stress dispersion are presented in papers [20, 22, 23]. According to [20], undrained shear strength can be determined by the formula

$$c_u = P \cdot \left[2 \cdot \pi \cdot \left(\sqrt{\frac{\sqrt{2} \cdot P}{p_{\epsilon}}} + 2 \cdot h_0 \cdot \tan \alpha_{\sigma} \right) \cdot \left(\sqrt{\frac{P}{2 \cdot \sqrt{2} \cdot p_{\text{tyre}}}} + 2 \cdot h_0 \cdot \tan \alpha_{\sigma} \right) \right]^{-1}, \quad (5)$$

where P – load upon the ground base surface, N; p_{tyre} – tyre pressure, Pa; h_0 – total thickness of the road pavement, m.

As follows from the equation (5), the tangent of an angle of dispersion is determined from the quadratic formula, i.e.

$$\tan \alpha_{\sigma 1,2} = \frac{-b \pm \sqrt{b^2 - 16 \cdot h_0^2 \cdot c}}{8 \cdot h_0^2}; \quad b = 2 \cdot h_0 \cdot \sqrt{\frac{P}{p_{\text{tyre}}}} \cdot \left(\frac{1}{\sqrt{2} \cdot \sqrt[4]{2}} + \sqrt[4]{2} \right);$$

$$c = P \cdot \left(\frac{1}{\sqrt{2} \cdot p_{\text{tyre}} - 2 \cdot \pi \cdot c_u} \right). \quad (6)$$

According to the results obtained in [22, 23], undrained shear strength is calculated from the formula which is similar to the relationship (4) and is written as

$$c_u = P \cdot \left[2 \cdot \pi \cdot \left(\sqrt{\frac{P}{p_{\text{tyre}}}} + 2 \cdot h_0 \cdot \tan \alpha_{\sigma} \right) \cdot \left(\sqrt{\frac{P}{2 \cdot p_{\text{tyre}}}} + 2 \cdot h_0 \cdot \tan \alpha_{\sigma} \right) \right]^{-1}. \quad (7)$$

Solving the equation (7) results in the following formulae

$$\tan \alpha_{\sigma 1,2} = \frac{-b \pm \sqrt{b^2 - 16 \cdot h_0^2 \cdot c}}{8 \cdot h_0^2}; \quad b = 2 \cdot h_0 \cdot \sqrt{\frac{P}{p_{\text{tyre}}}} \cdot \left(\sqrt{\frac{1}{2}} + 1 \right);$$

$$c = P \cdot \left(\frac{1}{\sqrt{2} \cdot p_{\text{tyre}} - 2 \cdot \pi \cdot c_u} \right). \quad (8)$$

J. Leng [16] suggests the formula similar to the relationships (6) and (8). It includes the amount of applied repeated loads in addition to the mentioned parameters and is written as

$$\tan \alpha_{\sigma} = \frac{\sqrt{(\sqrt{2}-1)^2 \cdot P_S / (2 \cdot p_{\text{tyre}}) + 2 \cdot P_S / (\lambda \cdot \pi \cdot c_u)} - (\sqrt{2}-1) \cdot P_S / (2 \cdot p_{\text{tyre}})}{6.5 \cdot \log N / c_u^{0.63}}, \quad (9)$$

where P_S – design axial load; c_u – undrained strength; N – design number of loads.

Formulae (5)–(9) have the same parameters but the results of their calculations are different. Therefore after performing unconsolidated-undrained triaxial tests and determining the undrained shear strength using relationships (6), (8) and (9), the angle of stress dispersion will be different with the same load parameters.

A procedure for calculating the angle of stress dispersion based on the direct measurements of the diameter of pressure distribution upon the plate located at a certain distance from the ground model surface is presented in work [24]. The procedure presupposes making a ground model with a standard compaction measuring device, with a paper leaf at a certain distance from the surface. The model surface is exposed to the force action with a rigid circular die to form an indentation cup on the ground surface. Then the soil is removed from the upper part of the sample so that to clean the paper leaf which also has an indentation cup of a larger size. The difference in the diameters of the indentation cups determines the distribution capacity, with the angle of stress dispersion being determined by the right triangle trigonometry. This procedure allows calculating values of an angle of stress dispersion for sandy and clay soils [24], but it cannot be used to calculate the one in soils reinforced with geosynthetics. The importance of calculating the angle of stress dispersion in ground bases reinforced with geosynthetics comes from the analysis of papers [22, 25–29] where the data on the angles of stress dispersion are different as well as conclusions concerning the positive influence of the reinforcement on the value of the angle of stress dispersion. The analysis of determining the angle of stress dispersion in reinforced and unreinforced soils is performed in the work [25]. The results are presented in Table 1.

Table 1. Angle of stress dispersion in reinforced and unreinforced ground bases [25, p. 729]

Researcher and a quotation source	Value of the angle of stress dispersion α_{σ}	
	Unreinforced ground base	Reinforced ground base
E.J. Barenberg [26]	$\alpha_{\sigma} = \arctan(0.3+5/h)$	$\alpha_{\sigma} = \arctan(0.6+5/h)$
J.P. Giroud and L. Noiray [22]	$\alpha_{\sigma} = \pi/4 - \varphi/2 = 45 - \varphi/2$	$\alpha_{\sigma} = 26.6-35$
Raumann G. [27]	$\alpha_{\sigma} = 28.8$	$\alpha_{\sigma} = 33$
J.B. Sellmeijer, C.J. Kenter and C. Van den Berg [28]	$\alpha_{\sigma} = 26.6-45$	$\alpha_{\sigma} = 26.6-45$
J.P. Love et al. [29]	–	$\alpha_{\sigma} = 26.6-31$

Note: h – depth of inserting an interlayer; it is the distance from the layer surface to the reinforcement horizon and it is usually the depth of a crushed-stone level, cm; φ – angle of internal friction, deg.

In order to begin the analysis of the data given in Table 1, it is necessary to point out that the table shows the values of the angles of stress dispersion in a base course being placed on the reinforcing interlayer.

The diagram illustrating the effect of such reinforcement is shown in Figure 2. According to the figure, the angle of stress dispersion in the unreinforced structure $\alpha_{\sigma 0}$ is less than that in the reinforced structure $\alpha_{\sigma 1}$. This effect is observed in the material over the reinforcing grid (for example, a crushed-stone level).

The tabular analysis shows that the authors of the paper [28] did not obtain the increase of the angle of stress dispersion while reinforcing the ground base, i.e. there was no effect described in Figure 2.

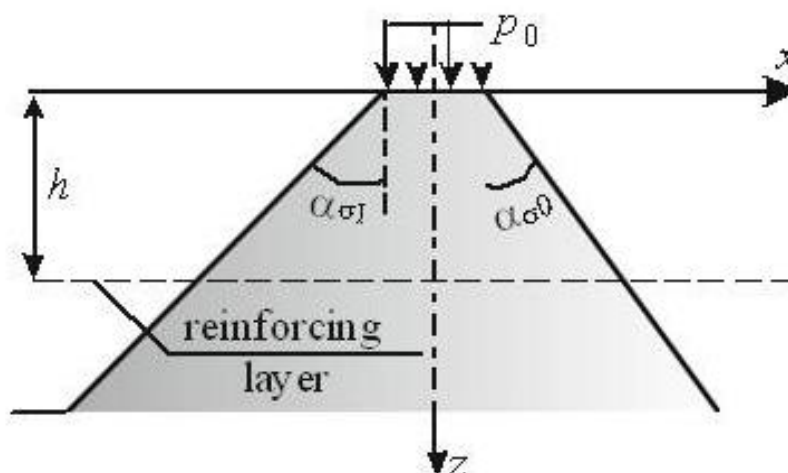


Figure 2. Diagram of different angles of stress dispersion in a reinforced and unreinforced layers

Some other researchers [22, 26, 27], on the contrary, provide values of angles of stress dispersion that proves the effect created. Since there is no single opinion about the effect of reinforcing shown in Figure 2, it can be assumed that the angle of stress dispersion increases in the material under the grid. There is a design diagram (Fig. 3) illustrating the reinforcement of a homogeneous ground base. A geogrid is placed within the layer of one and the same material, for example sand. According to this diagram, the angle of stress dispersion in the material under the grid increases in comparison with the analogous parameter of the same material over the grid.

Figure 3 introduces clarity into the traditional design diagram. Expediency of such a clarification should be proved experimentally. In this connection, it is necessary to calculate angles of stress dispersion in reinforced and unreinforced ground bases. Thus, a direct technique of measuring distribution capacity, that allows calculating angles of stress dispersion, is required. There are two reasons for it. First, it becomes possible to make a more precise calculation of angles of stress dispersion in reinforced and unreinforced ground bases if compared with the data in Table 1. Second, it is possible to explain the choice of a design diagram, for instance, Figure 2 or 3, or to suggest another design diagram being different from those presented in Figure 2 or 3.

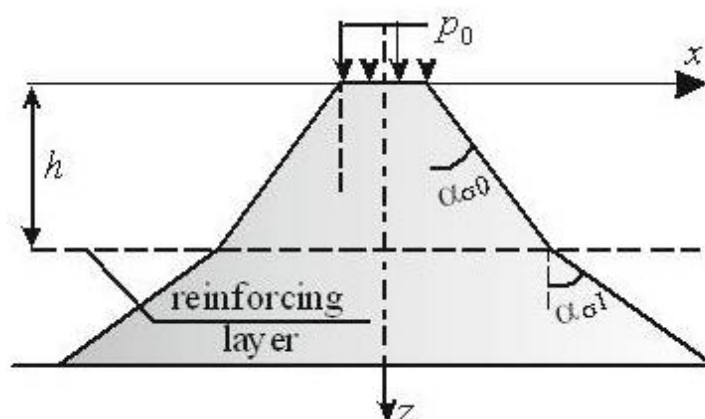


Figure 3. Diagram of different angles of stress dispersion in the material placed over and under the geogrid

Taking the foregoing into consideration, let us formulate the purpose and objectives of the research.

The purpose of this study is to investigate the distribution capacity of reinforced and unreinforced ground bases.

It can be done by achieving the following objectives:

1. Development of the direct method of measurement of reinforced and unreinforced ground bases distribution capacity, with the data being used to calculate an angle of stress dispersion.

Александров А.С., Калинин А.Л., Цыгулева М.В. Распределяющая способность песчаных грунтов, армированных геосинтетикой // Инженерно-строительный журнал. 2016. № 6(66). С. 35–48.

2. Application of mathematical statistics methods for calculating average and design values of angles of stress dispersion in reinforced and unreinforced ground bases.

3. Application of fitting criteria for comparing samplings of angles of stress dispersion in reinforced and unreinforced ground bases and for validating one of the design diagrams (Fig. 2 and Fig. 3).

Methods

The authors made a colour strip analysis to measure distribution capacity. The method had been chosen due to its pictorial presentation and its application for detecting slide curves trajectories in ground bases in master's [30] and doctoral [31] theses. An illustration of area elements of sliding surface obtained with the colour strip analysis can be seen in Figure 4. Arrows are used to show the slide curves being aligned with the trajectory of stress dispersion presented in Figures 1–3. This coincidence being taken into account, an angle of stress dispersion can be calculated by the right triangle trigonometry presented in Figure 4 (b).

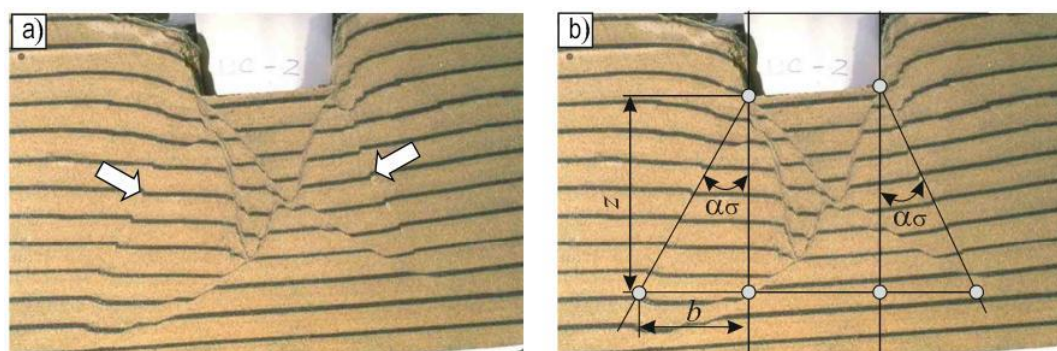


Figure 4. Sand base colour strip test:
a – general view of slide curves in a sand base [30];
b – chart for determining the angle of stress dispersion by the right triangle trigonometry

According to the analysis of Figure 4 (b) Kurdjumov method [32] can be used to calculate the angle of stress dispersion. The idea of this method is in soil photographing during the test, with the images being subsequently processed. It should be noted that the hypotenuse of the triangles passes through the points of colour strips breaks or next to them.

To perform the colour strip analysis models of reinforced and unreinforced ground bases were made, with fine sand being used as soil. Sand was compacted until the zero-air dry unit weight which was 98 % of the standard maximum dry density. It was necessary to determine the dry sand packed density to compact soil. A safety factor for compaction was calculated with the ratio of the required density to the dry sand packed density. The thickness of the sand layer to be obtained after leveling and, consequently, compacting was computed by multiplying of this safety factor and the layer thickness.

The model was made in layers. For the sand to be laid uniformly thread guide rails were used, with their height being equal to the thickness of the unconsolidated sand layer. The thread guide rails were arranged across an aquarium of the organic glass. Then the sand was laid between the thread guide rails and leveled with the bar moving along the rails. The sand layer having been leveled, the thread guide rails were carefully removed and some sand was added to fill the space.

The sand was compacted in two stages:

- at the beginning a roll-on of the layer was performed with a paint roller, the pressure from the hand gradually increasing while sand consolidating;
- to compact the sand finally a press with a rigid rectangular die put on the layer surface was used.

As for the criterion of the final compaction, it was a value of layer surface settling which was determined by the difference of the required thicknesses before and after compaction.

The model was made in a standard way, with layers of standard sand alternating with the coloured ones. Sand was coloured in green and blue. Different coloured stripes were arranged in alternation. For instance, the lower stripe was of green colour and the second one was blue. There were five layers of standard sand with four coloured stripes between them in the models.

A total of 15 models were manufactured. Five models are made without reinforcement, and 10 models produced by stacking two brands geosynthetics RD-60 75 × 75 and RD-60 100 × 100 into the model. Note that the reinforcing layer in road constructions carried out at the interface between the macadam and sand layers, in our models, this layer is laid in the sand. Laying geosynthetic reinforcement interlayer inside the sand is made to determine the scattering angles of stress above and below this layer. Laying geosynthetic materials performed on the surface of the third layer from the bottom of ordinary sand, and on top of it distributed sand, painted in green color. After laying and moistening colored sand his compaction was performed in the manner described above. At manufacturing the models applied criteria of geometric and the power of similarity. This allowed to define size of the stamp, the thickness of the sand layer. Table 2 shows the performance of physical and mechanical properties of the sand used in the model and compacted to the compaction factor of 0.98.

Table 2 Indicators of physical and mechanical properties of fine sand in the models of subgrade

№ sample	Indicators of physical properties, established by Russian standard GOST 5180-84 [24]				The mechanical properties and σ_3 at CN test without measuring the pore pressure		
	W, %	W/W _{opt}	$\rho_d, t/m^3$	$k = \rho_d / \rho_{dmax}$	σ_3 , kPa	c, kPa	$\varphi, ^\circ$
1	2	3	4	5	6	7	8
1 (kN)	9.33	0.94	1.85	0.98	50	3.3	36
2 (kN)					100		
3 (kN)					150		

Note: W – sand humidity; W_{opt} – optimum humidity; ρ_d – density of dry soil; k – compression ratio; ρ_{dmax} – maximum soil density in the standard device packing; σ_3 – the minimum principal stress in the device of triaxial compression when performing consolidated undrained test; c и φ – grip and angle of internal friction.

The essence of experimental method is reduced to the indentation the stamp into the surface of model and its deformation jointly with colored stripes. To transfer the load used the press GEOTECHAI-7000 LA 10 provided with the software package. For all models, the deformation rate was the same 3 mm/s. Pore pressure was not measured. During the test, we observe the change of location of the strips of colored sand. The load was applied so that the top 3 bands of colored sand receive noticeable deformation, and the fourth lower strip is not deformed. This allowed us to minimize the impact of the hard base on the deformation of sand in the model. With such character of the deformation color bars in reinforced models was possible to measure scattering angle in the upper part of the model, that is, over the reinforcing layer as well as the bottom of the model under geosynthetics. This allowed to draw a conclusion about the quantitative influence geosynthetic material on distributing ability of the sand. Then each model photographed for later processing photos with the help of computer programs to determine the scattering angles.

Computer programs were used for processing of photo images in order to perform linear measurements with an accuracy of up to 1 micron. In processing the results of the experiment in photographs set the location of the edges of the stamp and his axis of symmetry, which are shown by vertical lines I and II (Fig. 5).

Next determine the location of the lower border of the stamp, which is shown by the line III (Fig. 5). After this define position of start point uplift of sand on the surface of the color stripe, which corresponds to the intersection of the horizontal straight lines IV and V with vertical lines VI and VII (Fig. 5). The location of this point was fixed on picture by cross. Next perform location determination of point of an alleged gap of color strips. For this analyzed photographs test of works [30, 31], from which it follows that the most likely points of discontinuity of the color stripe are the point located in the middle of the deformed curved line segment, depicted vertical lines I and VI of, I and VII. At the Figure 5 these points signed C, D and E, F. To points C and D from the points corresponding the edges of the stamp – A and B held connecting them straight segments AC and BD, which indicate the locations the line of the stress distribution from the bottom of the stamp to the second color stripes, wherein in the models groups 1 and 3 are laid reinforcement geosynthetics. From the points C and D to the points E and F conducted segments CE and DF. These segments show the line of stress distribution between the second and third colored stripes.

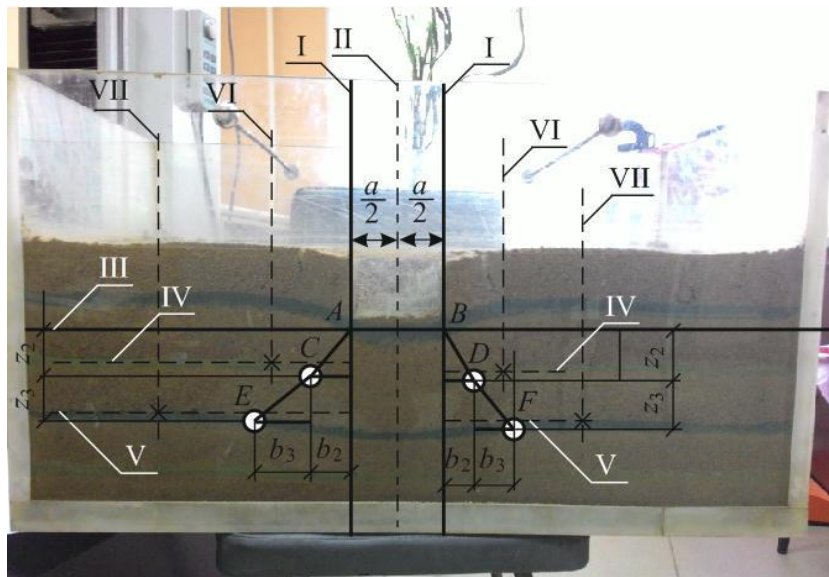


Figure 5. Scheme to the image processing model No. 11, belonging to the reinforced model sand base of group 3

Similar photos processing was made for the reinforced models. In Figure 5 there is an illustration of the processed pictures model No. 11, which analysis showed that the angles of scatter stress of the reinforcing mesh and underneath it are different. This fact confirmed the validity of the application to the calculation of reinforced soil bases the calculation scheme shown in Figure 3.

When processing the results of the test models of group 2, i.e. models of unreinforced sand foundation, it became clear that the segments AC and CE, as well as BD and DF are collinear or substantially coincide with it. It means in the unreinforced model stress distribution is limited to one line.

To determine scattering angles of the stress it is necessary to measure the length of the opposite and adjacent sides of a right triangle. In Figure 5 length of the opposite cathetus specified of length of b_2 and b_3 , and the length of the adjacent side – z_2 and z_3 . As the tangent of the angle in a right triangle is equal to ratio of the length of the opposite cathetus to the adjacent cathetus length, the scattering angles of the stress can be determined by the formulae:

$$\alpha = \arctg \frac{b_2}{z_2}; \quad \alpha = \arctg \frac{b_3}{z_3}. \quad (10)$$

Thus, for each colored band it is possible to determine two values of scattering angles of stress located on different sides of the stamp left and right respectively. This allowed for the reinforced models sandy grounds to form two sample scattering angles of stress.

The first sample contains 10 data points of scattering angles of stress α_{j1} characterizing distributing ability of sand over the reinforcing layer.

The second sample also includes 10 data points α_{j2} scattering angles stress, but characterize the ability to distributing sand under the reinforcing layer.

One sample of 20 private scattering angles of stress α_j is formed for unreinforced models.

Besides the processing of facsimiles direct measurements of all necessary sizes, illustrated in Figure 5, are used. In this case, all the lines which we are interested in were restored directly to the full-scale models and fixed by twine.

The initial position of the colored strips and the surface of the sand model were fixed before the test by applying labels to the ends of the aquarium. After the test the model, each label was used to secure the edges of the twine. Thus, the horizontal lines were restored. Restoration of vertical lines was performed with a plumb. Horizontal and vertical lines as well as the hypotenuse of right-angled triangles, which form together with the vertical cathetus, scattering angles stress, shown in Figure 6, was recovered in such manner.

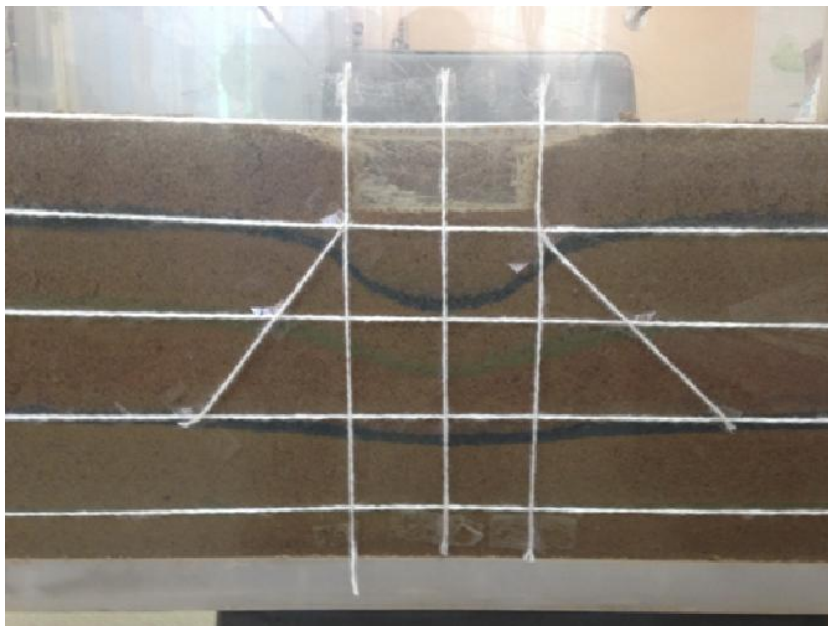


Figure 6. Recovered area stress distribution in the model No. 7, belonging unreinforced models of sand base of 2 group

Results and Discussion

Direct measurements of the size we are interested in was made by a metal line, which has a certificate of calibration. The measurement accuracy is 1 mm. Methods of calculating the scattering angles of stress analogous to the method applied in the processing of photographs. Despite the similarity of methods of measurement accuracy linear dimensions are different. Therefore, particular values of scattering angles, calculated from the results of direct measurements performed on a full-scale model, also grouped in five sample. At the first statistical processing of the data tested the possibility of combining the respective sample (samples 1 and 6, 2 and 7, 3 and 8, 4 and 9, 5 and 10) in a general population. For this purpose the Student's t -test and Fisher's F -test, following the standard procedure, were used.

Verifiable conditions of criteria have form:

$$t < t_{\alpha}; \quad F < F_{\alpha}, \quad (11)$$

where t_{α} – critical value of the Student distribution, also known as the coefficient of the normalized deviations accepted under bilateral confidence level of 0.95; F_{α} – the critical value of F -distribution.

The t and F criterion show that each pair of sample belongs to single corresponding general aggregate. Thus conclusion about the applicability of any developed by us techniques of measurement the linear size by means of which stress is calculated scattering angle can be done. For example, Table 3 shows the results of verification execution of the criteria (11) for sample No. 1 and No. 6, in which are grouped scattering angles stress in the upper part of the model group 1, in which the sand reinforced by mesh RD-60 75 x 75. Table 4 shows the results of verification execution of the criteria (11) for sample No. 2 and No. 7, in which are grouped the scattering angles stress in the bottom of the model group 1, in which the sand reinforced mesh by RD-60 75 x 75.

Table 3. Results of testing sample No. 1 and No. 6 on the appurtenance for one of the general population

Statistical characterization		Sample No. 1	Sample No. 6
Private values scattering angles of stress, °	1	39.41	40.40
	2	40.11	39.51
	3	39.85	39.74
	4	39.63	39.62
	5	38.70	38.69
	6	39.06	38.03
	7	38.80	39.43
	8	39.40	39.60
	9	39.76	39.78
	10	39.40	40.08
Mathematical expectation (middle sample), °		39.412	39.488
Root mean square deviation, °		0.45	0.46
Dispersion, grade ²		0.21	0.68
Statistics t		0.28	
The critical value of the Student's distribution t_{α}		2.26	
Statistics F		2.23	
The critical value of the distribution of R. Fischer F_{α}		3.18	
Checking conditions	$t < t_{\alpha}$	Performed as $0.28 < 2.26$	
	$F < F_{\alpha}$	Performed as $2.23 < 3.18$	
Conclusion: As a result of the implementation of both conditions criteria Student and Fisher sample No. 1 and No. 6 belong to the same general population			

Table 4. Results of testing sample No. 2 and No. 7 on the appurtenance for one of the general population

Statistical characterization		Sample No. 2	Sample No. 7
Private values scattering angles of stress, °	11	44.76	43.06
	12	44.59	44.39
	13	43.83	43.59
	14	43.66	43.59
	15	43.39	42.70
	16	42.41	43.57
	17	42.00	42.61
	18	43.12	43.04
	19	42.36	42.44
	20	41.99	41.75
Mathematical expectation (middle sample), °		43.211	43.074
Root mean square deviation, °		1.01	0.75
Dispersion, grade ²		1.03	0.56
Statistics t		0.33	
The critical value of the Student's distribution t_{α}		2.26	
Statistics F		1.84	
The critical value of the distribution of R. Fischer F_{α}		3.18	
Checking conditions	$t < t_{\alpha}$	Performed as $0.33 < 2.26$	
	$F < F_{\alpha}$	Performed as $1.84 < 3.18$	
Conclusion: As a result of the implementation of both conditions criteria Student and Fisher sample No. 2 and No. 7 belong to the same general population			

As the criteria (11) are satisfied, each pair of checked samples can be combined into one new sample for which to perform further statistical processing. Combining samples will increase the number of Aleksandrov A.S., Kalinin A.L., Tsyguleva M.V. Distribution capacity of sandy soils reinforced with geosynthetics. *Magazine of Civil Engineering*. 2016. No. 6. Pp. 35–48. doi: 10.5862/MCE.66.4

outcomes (partial values of scattering angles stress) in each new sample, whereby the quality of data will increase. After combining the samples of their total number was equal to 5. Samples 1 and 2 contain 20 particular values scattering angles stress in models of grounds reinforced with a mesh RD-60 75 × 75. The sample No. 1 contains scattering angles stresses on this grid, and the sample No. 2 shows the scattering angles stress under the grid. Sample No. 3 includes scattering angles of stress of unreinforced models. Sample 4 is similar to the sample 1, the sample 5 – sample 2, but samples No. 4 and No. 5 contains scattering angles of models of reinforced mesh RD-60 100 × 100.

New samples were tested for the presence of blunders, using as a criterion exceptions private values fulfillment of the condition Russian Standard GOST 20522-2012, then determined the estimated value of the scattering angles stress. In addition, the samples No. 1, No. 2, No. 3, No. 4 were verified to belong to the same general population. As a result, it was found that these samples are not subject to the unification. It follows therefrom that the factor of reinforcement of foundation soil is significant and results in increased scattering angles under the grid.

It was found that under the reinforcing mesh RD-60 100 × 100 scattering angle of stress increases by 2.9 %, while under the net of the RD-60 75 × 75 – increased by 9.1 %. This experimental fact suggests dependence on the effectiveness of the reinforcement from the grid cell size, made from one and the same material and having the same tensile strength.

To assess the reliability of the calculation scheme shown in Figure 2, it was performed statistical processing of private value of scattering angle of stress in sandy layers above the reinforcing grid and scattering angle of stress at the top of the unreinforced sand model. Performing of such statistical processing demanded the formation of four samples, each containing 20 private scattering angles of stress. The essence of the statistical processing involves estimating the possibility of combining the four samples in a general totality. Student's and Fisher's criteria, which we applied above, allow you to compare only two samples, for the assessment of belonging to the one general population three or more samples of these criteria are unfit. As far as number of private scattering angle of stress is identical in all four samples, rank criterion of Wilcoxon or rank criterion Kruskal–Wallis can be use.

In accordance with mathematical statistics literature data, Wilcoxon criterion is a nonparametric alternative to the Student criterion, which operates by comparing the total dispersion of two independent samples. Kruskal–Wallis criterion is a nonparametric alternative to the Fisher test. Kruskal–Wallis criterion is based on an assessment of the differences between the c medians ($c > 2$), and is a generalization of the Wilcoxon rank criterion. Therefore, we applied the criterion of Kruskal–Wallis test, which showed that the compound samples impossible. It follows that the reinforcement of the subgrade leads to a change in the scattering angle stress over the grid.

Thus, reinforcement of ground facilities leads to increased scattering angle of stress under a grid and some decrease this angle in the material located above the grid. This conclusion is confirmed by experiment refutes the calculation scheme shown in Figure 2 and confirms the circuit illustrated in Figure 3.

Table 5. Comparison of the results of determining the dispersion angle of the stress with those of other authors

Researcher and a quotation source	Expected value α_σ		The discrepancy results, %	
	Unreinforced ground base	Reinforced ground base	Unreinforced ground base	Reinforced ground base
According to the proposed method	39.45	43.14	–	–
J.P. Giroud and L. Noiray [19]	30	32.8	24	24
Raumann G. [24]	28.8	33	27	24
J.B. Sellmeijer, C.J. Kenter and C. Van den Berg [25]	35.5	42.5	10	1.5
J.P. Love et al. [26]	–	28.8	–	33.2

Analysis of the data Table 5 shows that in most cases the difference of the results is more than 20 %. This indicates that the application of the proposed methodology will improve the accuracy of the determination of this parameter of material.

Furthermore, the results publication can be applied to calculate the principal stresses. In order to do this the method proposed in [33] was used. The method lies in the fact that the minimum principal stress is defined as the percentage of the maximum principal stress. The formula has the form:

$$\sigma_2 = \sigma_3 = \alpha \cdot \xi \cdot \sigma_1, \quad (12)$$

where α – coefficient, which is a function of depth; ξ – lateral pressure coefficient.

The maximum principal stress can be represented by multiplication the pressure and the function reduce of its depth K . Applying this rule to the formula (1), for the cross section along the symmetry axis load we obtain:

$$\sigma_1 = \sigma_z = p \cdot K, \quad K = \left(1 + \frac{2 \cdot Z}{D_0} \cdot \operatorname{tg} \alpha_\sigma \right)^{-2}. \quad (13)$$

Function of depth α determined by the formula [33]:

$$\alpha = 1 - \sqrt{1 - K^2}. \quad (14)$$

Substituting additive (13) and (14) into the formula (12) allows getting model for determining the minimum principal stress:

$$\sigma_2 = \sigma_3 = p \cdot \xi \cdot \left(1 + \frac{2 \cdot Z}{D_0} \cdot \operatorname{tg} \alpha_\sigma \right)^{-2} \cdot \left(1 - \sqrt{1 - K^2} \right). \quad (15)$$

Thus, formulas (1) and (15) allow to calculate the main stresses for condition $\sigma_1 \geq \sigma_2 = \sigma_3$, which occurs in section along the symmetry axis of the load, distributed over the circular area. Therefore, it becomes possible to calculate the equivalent stresses on the various conditions of plasticity, including multi-surface modern conditions. Furthermore, according calculated to the relation (1) and (15) the principal stresses can be applied to calculate the residual strain on various mathematical models plastic deformation when subjected to repeated loads.

Conclusions

In conclusion, we can draw several inferences:

1. A method was developed direct measurement the distributing ability of reinforced and non-reinforced soil bases, based on the method of color stripe.
2. Calculation of scattering angle stress can be done one of two ways:
 - processing pictures with deformed colored stripes in accordance with the data in Figure 5.
 - restoration of essential lines, characterize the distributing ability on natural models, by performing the operation illustrated in Figure 6.
3. Statistical processing showed that the factor of the reinforcement of the sandy foundation is significant, that is affecting the value of the scattering angle stress in the materials located above the grid, as well as under it.
4. Under the Reinforcing Netting made of the same material, scattering angle of stress is increased by an amount depending on the cell size. It is found that the smaller the cell size, the greater the value of scattering angle of stress under the reinforcing grid.

References

1. Radovskiy B.S. Pervyye predstavleniya o prochnosti i raschete dorozhnykh odezhd: dorozhnyye odezhdy do XX veka [First perceptions about the strength and calculation of road pavements: pavement until the twentieth century]. *Dorozhnaya tekhnika*. 2012. Pp. 120–133. (rus)
2. Dolgikh G.V. *Raschet nezhestkikh dorozhnykh odezhd po kriteriyu bezopasnykh davleniy na grunty zemlyanogo polotna: diss...cand.tech.nauk*. [Calculation of nonrigid road pavements on the criterion of safe pressures in the soil subgrade. PhD Thesis]. Omsk: SibADI, 2014. 237 p. (rus)

Литература

1. Радовский Б.С. Первые представления о прочности и расчете дорожных одежд: дорожные одежды до XX века // *Дорожная техника*. 2012. С. 120–133.
2. Долгих Г.В. Расчет нежестких дорожных одежд по критерию безопасных давлений на грунты земляного полотна: дис. ... канд. техн. наук. Омск: СибАДИ, 2014. 237 с.
3. Taha El. Modelisation des deformation permanentes des graves non traitees. Application au calcul de l'ornierage des chaussees souples. PhD Thesis. Universite de Limoges, 2005. 173 p.

Aleksandrov A.S., Kalinin A.L., Tsyguleva M.V. Distribution capacity of sandy soils reinforced with geosynthetics. *Magazine of Civil Engineering*. 2016. No. 6. Pp. 35–48. doi: 10.5862/MCE.66.4

3. Taha El. Modelisation des deformation permanentes des graves non traitees. Application au calcul de l'ornierage des chaussees souples. PhD Thesis. Universite de Limoges, 2005. 173 p.
4. Dolgikh G.V. Eksperimentalnaya otsenka raspredelayayushchey sposobnosti glinistykh gruntov [Experimental estimation of distribution of the clay soils]. *Vserossiyskaya 65-ya nauchno-tekhnicheskaya konferentsiya FGBOU VPO «SibADI» [Proceedings of 65th scientific technical conference in SibADI]*. Omsk: FGBOU VPO SibADI, 2011. Pp. 48–54. (rus)
5. Aleksandrov A.S., Aleksandrova N.P., Dolgikh G.V. Modifitsirovannyye modeli dlya rascheta glavnykh napryazheniy v dorozhnykh konstruktsiyakh iz diskretnykh materialov [Modified model for calculation of the principal stresses in road constructions of discrete materials]. *Stroitelnyye materialy*. 2012. No. 10. Pp. 14–17. (rus)
6. Aleksandrova N.P., Semenova T.V., Dolgikh G.V. Sovershenstvovaniye modeley rascheta glavnykh napryazheniy i deviatora v grunte zemlyanogo polotna [Development of models to calculate the principal stresses and deviator in the soil subgrade]. *Vestnik SibADI*. 2014. No. 2(36). Pp. 49–54. (rus)
7. Odemark N. Investigations as to the elastic properties of soils and design of pavements according to the theory of elasticity. *Medclelande*. 1949. Vol. 77. Pp. 43–52.
8. Lee Y.-H. Study of backcalculated pavement layer moduli from the LTPP database. *Journal of Science and Engineering*. 2010. Vol. 13. No. 2. Pp. 145–156.
9. Fi I., Szentpéteri I. A mechanistic-empirical approach for asphalt overlay design of asphalt pavement structures. *Civil Engineering*. 2014. Vol. 58/1. Pp. 55–62.
10. Horak E., Hefer A., Maina J. Determination of pavement number for flexible pavements using fwd deflection bowl information. *Proceedings of the 34th Southern African Transport Conference (SATC 2015)*. 2015. Pp. 187–200.
11. Burd H.J., Frydman S. Bearing capacity of plane-strain footings on layered soils. *Canadian Geotechnical Journal*. 1997. Vol. 34. Pp. 241–253.
12. Meyer N., Elias J.M. Design methods for roads reinforced with multifunctional geogrid composites for sub-base stabilization. *German Conference on Geosynthetics*. Munich: Technical University Munich, 1999. Pp. 1–8.
13. Benjamin C.V.S., Bueno B., Zornberg J.G. Field monitoring evaluation of geotextile-reinforced soil retaining walls. *Geosynthetics International Journal*. 2007. Vol. 14. No. 2. Pp. 100–118.
14. Bueno B.S., Costanzia M.A., Zornberg J.G. Conventional and accelerated creep tests on nonwoven needle-punched geotextiles. *Geosynthetics International*. 2005. Vol. 12. No. 6. Pp. 276–287.
15. Hu Y.C., Zhang Y.M. Analysis of load-settlement relationship for unpaved road reinforced with geogrid. *First International Symposium on Geotechnical Safety & Risk*. 2007. Pp. 609–615.
16. Leng J. *Characteristics and behavior of geogrid-reinforced aggregate under cyclic load*. PhD Thesis. Raleigh, 2002. 152 p.
17. Mounes S.M. An overview on the use of geosynthetics in pavement structures. *Scientific Research and Essays*. 2011. No. 6(11). Pp. 2234–2241.
18. Zornberg J.G., Gupta R. Geosynthetics in pavements: North American contributions. *9th International Conference on Geosynthetics*. Guarujá, Brazil, 2010. Pp. 379–398.
19. Badanin A.N., Bugrov A.K., Krotov A.V. Obosnovaniye pervoy kriticheskoy nagruzki na zernistuyu sredy supeschanogo osnovaniya [The determination of the first critical load on particulate medium of sandy loam foundation]. *Magazine of Civil Engineering*. 2012. No. 9(35). Pp. 29–34. (rus)
20. Koerner R.M. *Designing with geosynthetics. Fifth edition*. Upper Saddle River. New Jersey, 2005. 796 p.
4. Долгих Г.В. Экспериментальная оценка распределяющей способности глинистых грунтов // Всероссийская 65-я научно-техническая конференция ФГБОУ ВПО «СибАДИ». Омск: ФГБОУ ВПО «СибАДИ», 2011. С. 48–54.
5. Александров А.С., Александрова Н.П., Долгих Г.В. Модифицированные модели для расчета главных напряжений в дорожных конструкциях из дискретных материалов // Строительные материалы. 2012. № 10. С. 14–17.
6. Александрова Н.П., Семенова Т.В., Долгих Г.В. Совершенствование моделей расчета главных напряжений и девиатора в грунте земляного полотна // Вестник СибАДИ. 2014. № 2(36) С. 49–54.
7. Odemark N. Investigations as to the elastic properties of soils and design of pavements according to the theory of elasticity // *Medclelande*. 1949. Vol. 77. Pp. 43–52.
8. Lee Y.-H. Study of backcalculated pavement layer moduli from the LTPP database // *Journal of Science and Engineering*. 2010. Vol. 13. No. 2. Pp. 145–156.
9. Fi I., Szentpéteri I. A mechanistic-empirical approach for asphalt overlay design of asphalt pavement structures // *Civil Engineering*. 2014. Vol. 58/1. Pp. 55–62.
10. Horak E., Hefer A., Maina J. Determination of pavement number for flexible pavements using fwd deflection bowl information // *Proceedings of the 34th Southern African Transport Conference (SATC 2015)*. 2015. Pp. 187–200.
11. Burd H.J., Frydman S. Bearing capacity of plane-strain footings on layered soils // *Canadian Geotechnical Journal*. 1997. Vol. 34. Pp. 241–253.
12. Meyer N., Elias J.M. Design methods for roads reinforced with multifunctional geogrid composites for sub-base stabilization // *German Conference on Geosynthetics*. Munich: Technical University Munich, 1999. Pp. 1–8.
13. Benjamin C.V.S., Bueno B., Zornberg J.G. Field monitoring evaluation of geotextile-reinforced soil retaining walls // *Geosynthetics International Journal*. 2007. Vol. 14. No. 2. Pp. 100–118.
14. Bueno B.S., Costanzia M.A., Zornberg J.G. Conventional and accelerated creep tests on nonwoven needle-punched geotextiles // *Geosynthetics International*. 2005. Vol. 12. No. 6. Pp. 276–287.
15. Hu Y.C., Zhang Y.M. Analysis of load-settlement relationship for unpaved road reinforced with geogrid // *First International Symposium on Geotechnical Safety & Risk*. 2007. Pp. 609–615.
16. Leng J. *Characteristics and behavior of geogrid-reinforced aggregate under cyclic Load*. PhD Thesis. Raleigh, 2002. 152 p.
17. Mounes S.M. An overview on the use of geosynthetics in pavement structures // *Scientific Research and Essays*. 2011. No. 6(11). Pp. 2234–2241.
18. Zornberg J.G., Gupta R. Geosynthetics in pavements: North American contributions // *9th International Conference on Geosynthetics*. Guarujá, Brazil, 2010. Pp. 379–398.
19. Баданин А.Н., Бугров А.К., Кротов А.В. Обоснование первой критической нагрузки на зернистую среду супесчаного основания // Инженерно-строительный журнал. 2012. № 9(35). С. 29–34.
20. Koerner R.M. *Designing with geosynthetics. Fifth edition*. Upper Saddle River, New Jersey, 2005. 796 p.
21. Клейн Г.К. *Строительная механика сыпучих тел*. М.: Стройиздат, 1977. 256 с.
22. Giroud J.P., Noiray L. Geotextile-reinforced unpaved road design // *Journal of Geotechnical Engineering, ASEC*. 1981. Vol. 107. Pp. 1233–1254.
23. Giroud J.P., Ah-Line C., Bonaparte R. Design of unpaved roads and trafficked areas with geogrids // *Proceedings of the symposium on polymer grid reinforcement in civil engineering*. London, 1984. Pp. 116–127.
24. Александров А.С., Александрова Н.П., Кузин Н.В.,

Александров А.С., Калинин А.Л., Цыгулева М.В. Распределяющая способность песчаных грунтов, армированных геосинтетикой // Инженерно-строительный журнал. 2016. № 6(66). С. 35–48.

21. Kleyn G.K. Stroitel'naya mekhanika sypuchikh tel [Structural theory of granular materials]. Moscow: Stroyizdat, 1977. 256 p.
22. Giroud J.P., Noiray L. Geotextile-reinforced unpaved road design. *Journal of Geotechnical Engineering, ASEC*. 1981. Vol. 107. Pp. 1233–1254.
23. Giroud J.P., Ah-Line C., Bonaparte R. Design of unpaved roads and trafficked areas with geogrids. *Proceedings of the symposium on polymer grid reinforcement in civil engineering*. London, 1984. Pp. 116–127.
24. Aleksandrov A.S., Aleksandrova N.P., Kuzin N.V., Dolgikh G.V. Issledovaniye vertikalnykh napryazheniy v zemlyanom polotne s uchetom raspredelyayushchey sposobnosti gruntov [Study of vertical stresses in the subgrade with account of the distribution capacity of soils]. *Transportnoye stroitel'stvo*. 2010. No. 8. Pp. 18–21. (rus)
25. Espinoza R.D., Bray J.D. An integrated approach to evaluating single-layer reinforced soils. *Geosynthetics International*. 1995. Vol. 2. No. 4. Pp. 723–739.
26. Barenberg E.J. *Design procedures for soil-fabric-aggregate systems with Mirafi 500X fabric*. PhD Thesis. Department of Civil Engineering. University of Illinois, USA. 1980. 26 p.
27. Raumann G. Geotextiles in unpaved roads: design considerations // *Proceedings of the second international conference on geotextiles*. Las Vegas, 1982. Vol. 2. Pp. 417–422.
28. Sellmeijer J.B., Kenter C.J., Van den Berg C. Calculation method for fabric reinforced road // *Proceedings of the second international conference on geotextiles*. Las Vegas, 1982. Vol. 2. Pp. 393–398.
29. Love J.P. Analytical and model studies of reinforcement of a layer of granular fill on soft clay subgrade // *Canadian Geotechnical Journal*. 1987. Vol. 24. No. 4. Pp. 611–622.
30. Мельников А.В. Исследование прочности и деформируемости слабых грунтов оснований, усиленных ар-мированием: дис. ... магистра техники и технологии строительства / Пензенский государственный университет архитектуры и строительства. Пенза, 2012. 216 с.
31. Королев К.В. Несущая способность оснований в стабилизированном и нестабилизированном состоянии: дис. ... д-ра техн. наук. Новосибирск, 2014. 325 с.
32. Христов Х. Санкт-Петербург, 1889 г.: первое фотографическое исследование процесса разрушения грунта под фундаментом // *Реконструкция городов и геотехническое строительство*. 2003. № 7. С. 187–192.

Anatoliy Aleksandrov,
+7(913)6164212; Aleksandrov00@mail.ru

Aleksandr Kalinin,
+7(965)9858572; a1exandr55ne@mail.ru

Margarita Tsyguleva,
+7(381)2651563; m.v.tsyguleva@gmail.com

Анатолий Сергеевич Александров,
+7(913)6164212;
эл. почта: Aleksandrov00@mail.ru

Александр Львович Калинин,
+7(965)9858572;
эл. почта: a1exandr55ne@mail.ru

Маргарита Викторовна Цыгулева,
+7(381)2651563;
эл. почта: m.v.tsyguleva@gmail.com

© Aleksandrov A.S., Kalinin A.L., Tsyguleva M.V., 2016